Molecular Plant
Research Article

CellPress
PARTNER JOURNAL

A Plant Immune Receptor Degraded by Selective Autophagy

Fan Yang[1,2], Athen N. Kimberlin[2,3,5], Christian G. Elowsky[4], Yunfeng Liu[2,6], Ariadna Gonzalez-Solis[2,3], Edgar B. Cahoon[2,3,*] and James R. Alfano[1,2,*]

[1]Department of Plant Pathology, University of Nebraska, Lincoln, NE 68588-0722, USA

[2]Center for Plant Science Innovation, University of Nebraska, Lincoln, NE 68588-0660, USA

[3]Department of Biochemistry, University of Nebraska, Lincoln, NE 68588-0664, USA

[4]Center for Biotechnology, University of Nebraska, Lincoln, NE 68588-0665, USA

[5]Present address: Department of Biochemistry, University of Missouri, Columbia, MO 65211, USA

[6]Present address: College of Life Science and Technology, University of Guangxi, Nanning 530004, China

***Correspondence: Edgar B. Cahoon (ecahoon2@unl.edu), James R. Alfano (jalfano2@unl.edu)**

https://doi.org/10.1016/j.molp.2018.11.011

ABSTRACT

Plants recycle non-activated immune receptors to maintain a functional immune system. The *Arabidopsis* immune receptor kinase FLAGELLIN-SENSING 2 (FLS2) recognizes bacterial flagellin. However, the molecular mechanisms by which non-activated FLS2 and other non-activated plant PRRs are recycled remain not well understood. Here, we provide evidence showing that *Arabidopsis* orosomucoid (ORM) proteins, which have been known to be negative regulators of sphingolipid biosynthesis, act as selective autophagy receptors to mediate the degradation of FLS2. *Arabidopsis* plants overexpressing ORM1 or ORM2 have undetectable or greatly diminished FLS2 accumulation, nearly lack FLS2 signaling, and are more susceptible to the bacterial pathogen *Pseudomonas syringae*. On the other hand, *ORM1/2* RNAi plants and *orm1* or *orm2* mutants generated by the CRISPR/Cas9-mediated gene editing have increased FLS2 accumulation and enhanced FLS2 signaling, and are more resistant to *P. syringae*. ORM proteins interact with FLS2 and the autophagy-related protein ATG8. Interestingly, overexpression of *ORM1* or *ORM2* in autophagy-defective mutants showed FLS2 abundance that is comparable to that in wild-type plants. Moreover, FLS2 levels were not decreased in *Arabidopsis* plants overexpressing ORM1/2 derivatives that do not interact with ATG8. Taken together, these results suggest that selective autophagy functions in maintaining the homeostasis of a plant immune receptor and that beyond sphingolipid metabolic regulation ORM proteins can also act as selective autophagy receptors.

Key words: *Plant immunity*, selective autophagy, pattern recognition receptor, selective autophagy receptors

Yang F., Kimberlin A.N., Elowsky C.G., Liu Y., Gonzalez-Solis A., Cahoon E.B., and Alfano J.R. (2019). A Plant Immune Receptor Degraded by Selective Autophagy. Mol. Plant. **12**, 113–123.

INTRODUCTION

Plants are in constant contact with both pathogenic and beneficial microorganisms. Cell surface immune pattern-recognition receptors (PRRs) detect the presence of invading microbes by recognizing conserved microbial molecules known as pathogen- or microbe-associated molecular patterns (PAMPs/MAMPs) (Couto and Zipfel, 2016). The perception of PAMPs by PRRs leads to pattern-triggered immunity, which can restrict pathogen ingress. *Arabidopsis* PRR FLAGELLIN-SENSING 2 (FLS2) recognizes bacterial flagellin (or its epitope flg22) (Couto and Zipfel, 2016). Flagellin-bound FLS2 becomes activated and is endocytosed into the plant cell, a process that is thought to be coupled with activation of FLS2 signaling (Robatzek et al., 2006). Attenuation of FLS2 activation occurs upon recruitment of the U-box ubiquitin ligases PUB12 and PUB13 to the FLS2 complex. PUB12 and PUB13 polyubiquitinate FLS2, promoting FLS2 degradation, leading to turnover of activated FLS2 (Lu et al., 2011). To maintain functional and stable levels of FLS2 at the cell surface, non-activated FLS2 (not bound to its flagellin ligand) is constitutively recycled via endosomal trafficking, a process that is distinct from endosomal trafficking of activated FLS2 (Beck et al., 2012). The molecular mechanisms by which non-activated

Published by the Molecular Plant Shanghai Editorial Office in association with Cell Press, an imprint of Elsevier Inc., on behalf of CSPB and IPPE, SIBS, CAS.

FLS2 and other non-activated plant PRRs are recycled remain not well understood.

Orosomucoid (ORM) proteins, known negative regulators of sphingolipid biosynthesis, suppress the activity of serine palmitoyltransferase (SPT), the first and rate-limiting enzyme in the sphingolipid synthesis pathway (Breslow et al., 2010; Han et al., 2010). In *Arabidopsis*, ORM proteins encoded by two genes, *ORM1* (At1g01230) and *ORM2* (At5g42000), were recently shown to localize to the endoplasmic reticulum (ER) and other subcellular locations, including the cytosol, to control sphingolipid homeostasis (Kimberlin et al., 2013, 2016; Li et al., 2016). Overexpression of *ORMs* can inhibit SPT activity without affecting sphingolipid accumulation in *Arabidopsis*. Recently, it was reported that an *Arabidopsis orm1 ORM2* RNAi knockdown plant (lacking ORM1 with reduced amounts of ORM2) showed increased sensitivity to oxidative stress. Interestingly, *orm1 ORM2* RNAi plants displayed significantly increased resistance against the bacterial pathogen *Pseudomonas syringae* (Li et al., 2016), but the mechanism by which ORMs increase such resistance is not known.

ORM genes also affect mammalian immune responses through different mechanisms. Downregulation of human orosomucoid-like 1 (ORMDL1) decreases the abundance of non-activated Toll-like receptor 4 (TLR4), while knockdown of ORMDL2 increases lipopolysaccharide-induced internalization of TLR4 from the plasma membrane into endosomes (Koberlin et al., 2015). It is generally believed that altered membrane lipid composition is responsible for ORMDL1/2-mediated TLR4 signaling and trafficking. Dysregulation of the ORMDL3 gene is associated with several autoimmune diseases, including asthma and type 1 diabetes (Das et al., 2017). Recent studies have shown that ORMDL3-mediated expression of autophagy-related genes, as well as overexpression of ORMDL3, induce autophagy and suppress B lymphocyte development (Ma et al., 2015; Dang et al., 2017). Thus, human ORMDLs regulate diverse immune responses through sphingolipid-dependent and autophagy-dependent signaling pathways.

Autophagy is a major cellular degradation process by which distinct cytoplasmic components are sequestered and transported into vacuoles in plants (lysosomes in animals) for breakdown and eventual recycling (Wong and Maclachlan, 1980; Farre and Subramani, 2016; Michaeli et al., 2016; Marshall and Vierstra, 2018). This catabolic process is conserved in all eukaryotes, and a core set of autophagy-related (ATG) proteins, which cooperate in forming and regulating autophagic machinery, has been identified. Autophagy was initially considered to be a non-specific self-consumption process induced by nutrient starvation. However, it is now clear that autophagy can regulate cellular homeostasis by selectively degrading specific cargo materials. The specificity of cargo is determined by selective autophagy receptors, which function as sorting adaptors that recruit selected cargo into double-membrane compartments known as autophagosomes, through their ability to interact with ATG8 proteins (Stolz et al., 2014). Specific interactions between selective autophagy receptors and ATG8 require the ATG8-interacting motif (AIM), a short motif within the selective autophagy receptor.

In this study, we show that *Arabidopsis* ORM1 and ORM2 modulate plant immunity by regulating FLS2 protein accumulation. RNAi-mediated downregulation of *ORM* expression and mutations in *ORM1* or *ORM2* specifically enhance FLS2-dependent immune responses and increase the abundance of FLS2. Conversely, overexpression of *ORMs* causes FLS2 degradation and abrogates FLS2-dependent signaling. We found that ORMs possess AIMs that are required for each ORM to interact with ATG8 and that each ORM binds to FLS2. Our findings suggest that ORMs function as selective autophagy receptors for FLS2 cargo and suggest a broader role for ORM proteins beyond sphingolipid metabolic regulation.

RESULTS

ORMs Specifically Affect FLS2 Signaling

To determine whether ORM proteins contribute to plant immunity, we inoculated the bacterial pathogen *P. syringae* pv. *tomato* (*Pto*) DC3000 on wild-type *Arabidopsis thaliana* ecotype Columbia (Col-0) plants, Col-0 ORM RNA-silenced (*ORM* RNAi) lines, and Col-0 plants that overexpress ORM1 or ORM2 (Kimberlin et al., 2016) (Supplemental Figure 1A and 1B). The latter plants exhibited more severe disease symptoms and increased bacterial colonization compared with wild-type plants (Figure 1A and 1B). In contrast, the *Arabidopsis ORM1* and *ORM2* RNAi plants (with greatly reduced levels of *ORM1* and *ORM2* RNA, respectively) exhibited milder disease symptoms and reduced bacterial colonization (Figure 1A and 1B). *In planta* growth of non-pathogenic *Pto* DC3000 Δ*hrcC* was promoted in plants overexpressing ORM1 or ORM2, but restricted in both *ORM* RNAi lines (Supplemental Figure 1C). To elucidate how ORM proteins enhance pathogen growth and promote disease, we evaluated immunity in *ORM* RNAi and ORM-overexpressing plants. FLS2 is a well-studied *Arabidopsis* PRR that contributes to immunity to *P. syringae* (Kunze et al., 2004). *ORM* RNAi plants treated with flg22, an immunogenic epitope of flagellin, accumulated more callose deposits and produced more reactive oxygen species (ROS) than wild-type *Arabidopsis*, whereas lower levels of both were detected in plants overexpressing ORM1 or ORM2 (Figure 1C and 1D; Supplemental Figure 2A). Additionally, the expression of flg22-induced immunity-related genes was increased in *ORM* RNAi plants but greatly inhibited in plants overexpressing ORM1 or ORM2 (Figure 1E). The inhibition of immunity in plants overexpressing ORM proteins appeared to be specific to FLS2 because other PAMP-induced immune responses were unaffected (Supplemental Figure 2B and 2D), suggesting that ORMs negatively regulate FLS2 signaling, but not other PRR signaling pathways, and promote *P. syringae* pathogenesis.

Overexpression of *ORMs* Diminishes FLS2 Accumulation

FLS2 immune signaling is coupled with internalization of FLS2 from the plasma membrane into endosomes upon flagellin or flg22 binding (Robatzek et al., 2006). To determine whether ORM proteins affect FLS2 internalization, we transformed an *Arabidopsis* line expressing GFP-tagged FLS2 (Robatzek et al., 2006) with genes encoding ORM1-HA (hemagglutinin tag) or ORM2-HA. Prior to flg22 treatment, we found uniform GFP signal at the cell surface or in the cytoplasm of epidermal cells in control plants and plants overexpressing ORM1-HA or ORM2-HA (Figure 2A). After treatment, FLS2-GFP internalization was observed in the control plants but not in the ORM1/2-HA overexpression lines, which

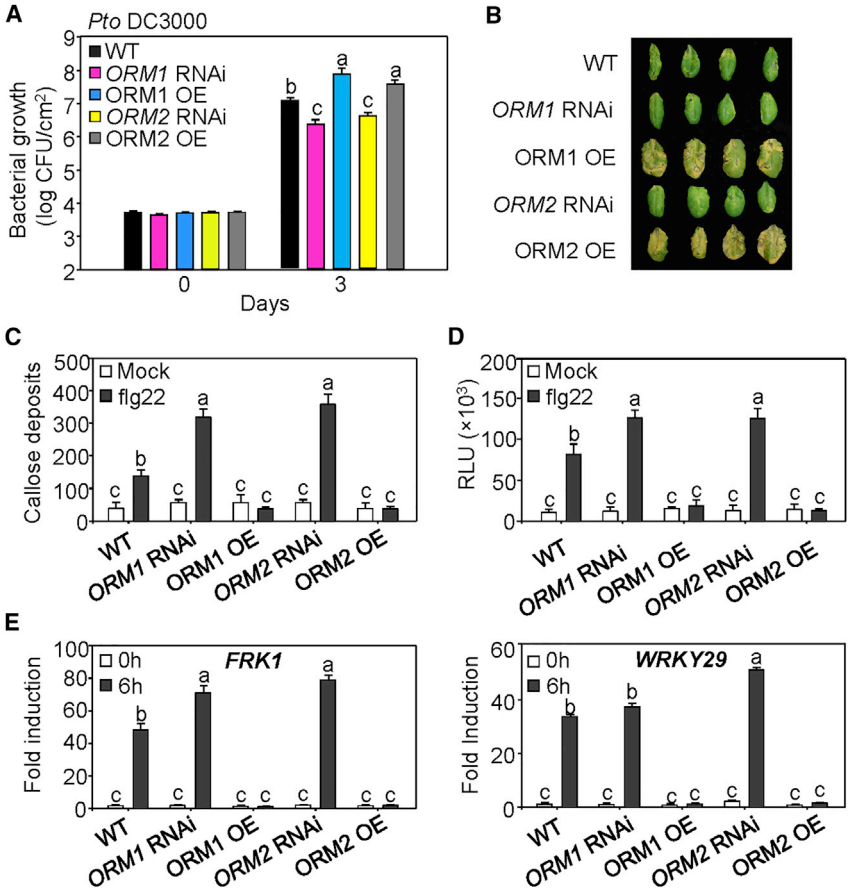

Figure 1. ORM Proteins Affect Plant Susceptibility to *Pseudomonas syringae* and FLS2 Signaling.

(A) *P. syringae* pathogenicity assays on wild-type *A. thaliana* Col-0 (WT), transgenic plants overexpressing ORM1 or ORM2, and *ORM1* or *ORM2* RNAi knock-down lines. Plants were infiltrated with *P. syringae tomato* DC3000 (*Pto* DC3000). Bacterial growth was determined 3 days after spray inoculation. Values are shown as mean ± SE. $n = 4$ biological replicates; experiments were repeated three times with similar results.

(B) Disease symptom production after 4 days in plants depicted in **(A)**.

(C) Quantification of callose deposits. Values are mean ± SE ($n = 18$).

(D) Reactive oxygen species (ROS) production (RLU, relative luminescence unit; $n = 12$) in WT and ORM transgenic plants treated with 1 μM flg22 or water as a mock control. Experiments were repeated three times.

(E) Flg22-induced gene expression in WT and ORM transgenic plants. Leaves infiltrated with 1 μM flg22 were sampled at 0 and 6 h post treatment, and gene expression was measured using qRT–PCR. Values are mean ± SE, $n = 3$ technical replicates.

Experiments were repeated three times with similar results. Different letters in the graphs indicate statistical significance between treatments (one-way ANOVA with Tukey's test; $P < 0.01$).

exhibited a diffuse GFP signal along the plasma membrane and/or cytosol. We next analyzed levels of FLS2-GFP in these plants without flg22 treatment and found free GFP, but not full-length FLS2-GFP, in plants overexpressing ORM proteins (Figure 2B). This finding suggests that the GFP signal observed in FLS2-GFP ORM1/2-HA plants (Figure 2A) was due to GFP, not to FLS2-GFP. To further investigate the apparent reduction of FLS2 levels, we made transgenic *Arabidopsis* plants expressing ORM1-HA or ORM2-HA under the control of the constitutive CaMV 35S promoter. Native FLS2 accumulation was greatly reduced in independent lines overexpressing ORM1/2-HA (Figure 2C). These plant lines also lacked FLS2 signaling, based on greatly reduced callose deposition and ROS production after flg22 treatment (Supplemental Figure 3A and 3B). To confirm this result, we also generated transgenic *Arabidopsis* Col-0 lines expressing either ORM1-HA or ORM2-HA under the control of an estradiol-inducible promoter. Plants expressing ORM1-HA or ORM2-HA that had been treated with estradiol had reduced amounts of FLS2 (Figure 2D) and produced less ROS after flg22 treatment (Supplemental Figure 3C).

We next sought to determine the abundance of FLS2 in *Arabidopsis ORM* RNAi plants and found slightly higher FLS2 protein levels in these plants compared with wild-type plants (Figure 2E). Importantly, FLS2 RNA levels were not significantly different in *ORM* overexpression, *ORM* RNAi, and wild-type *Arabidopsis* plants (Supplemental Figure 3D), indicating that the differences in FLS2 protein levels were not due to *FLS2* transcription levels. To further validate these observations, we mutated the *Arabidopsis ORMs* using the CRISPR/Cas9 approach. Like *ORM* RNAi plants, the CRISPR *orm1* and *orm2* mutants accumulated more FLS2 and exhibited enhanced flg22-triggered ROS production compared with wild-type plants (Figure 2F and Supplemental Figure 3E–3G). The CRISPR *orm* mutants proved to be more resistant than the *ORM* RNAi lines against *Pto* DC3000 infection, likely because the *orm* mutants have slightly higher amounts of FLS2 than the *ORM* RNAi lines (Supplemental Figure 3H). We were unable to isolate a CRISPR *orm1 orm2* double mutant, suggesting that such a mutant is lethal. Collectively, these results indicate that ORM proteins can reduce FLS2 protein levels.

To determine whether the differences in *Pto* DC3000 pathogenicity observed in *Arabidopsis* plants overexpressing ORM1/2 and in RNAi lines with diminished levels of *ORM1/2* RNA were due to FLS2 activation, we inoculated these plants with a *Pto* DC3000 Δ*fliC* mutant that lacks flagellin and, therefore, does not trigger FLS2 signaling. Importantly, the growth of the *Pto* DC3000 Δ*fliC* mutant on these plants and the disease symptoms produced were similar to those observed on wild-type *Arabidopsis* (Figure 2G). This suggests that the observed ORM1/2-dependent differences in *Pto* DC3000 pathogenicity (Figure 1A and 1B) were due primarily to FLS2-induced plant immunity.

ORM-Dependent Reduction in FLS2 Levels Is Dependent on FLS2 Internalization

Transient expression of FLS2-GFP with ORM1-HA or ORM2-HA in *Nicotiana benthamiana* also resulted in reduced amounts of

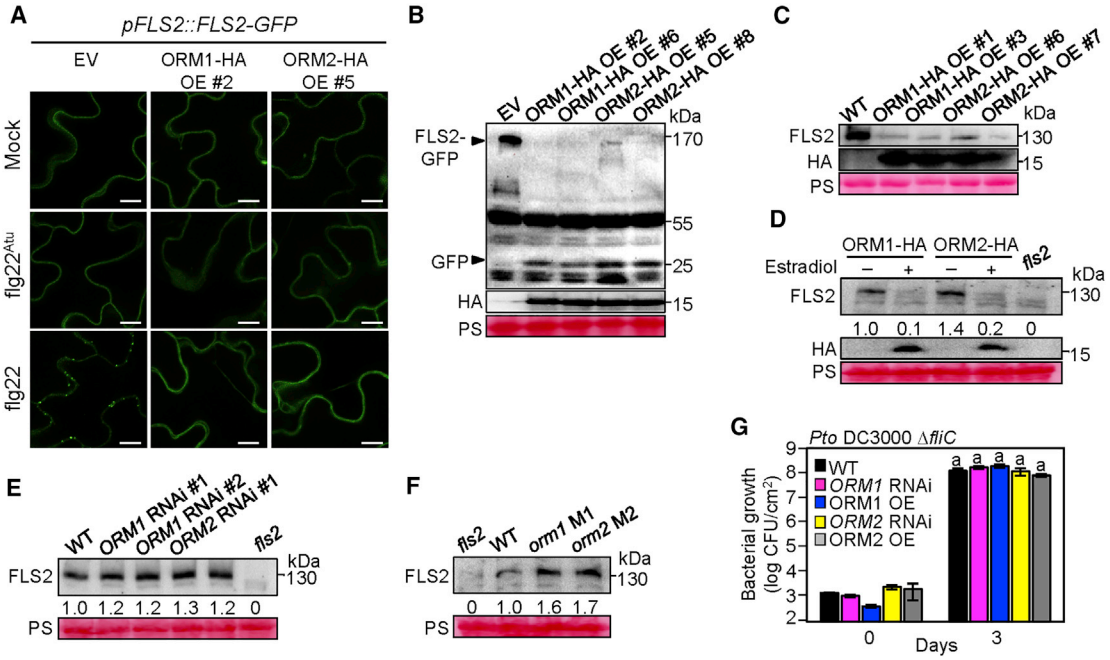

Figure 2. ORM Expression Levels Are Important for FLS2 Protein Accumulation.

(A) Confocal microscopy of 3-week-old *A. thaliana Col-0* (*FLS2p*::*FLS2-3xmyc-GFP*) plants expressing ORM1-HA (line #2) or ORM2-HA (line #5) treated with water (mock), 10 μM inactive flg22^{Atu}, or 10 μM flg22 for 40 min prior to imaging. Scale bars, 10 μm.

(B) Immunoblot analysis of FLS2-GFP and free GFP in plant lines expressing ORM1-HA or ORM2-HA.

(C) Immunoblot analysis of endogenous FLS2 in wild-type (WT) *Arabidopsis* Col-0 and independent Col-0 lines overexpressing ORM1-HA or ORM2-HA.

(D) Immunoblot analysis of endogenous FLS2 in *Arabidopsis* expressing ORM1-HA or ORM2-HA under the control of an estradiol-inducible promoter.

(E) Immunoblot analysis of endogenous FLS2 in WT and *ORM* RNAi plants. In **(D)** and **(E)**, An *fls2* mutant lacking FLS2 was added as a control.

(F) Immunoblot analysis of endogenous FLS2 in the *orm* mutants and WT plants. Numbers underneath immunoblot lanes represent FLS2 abundance relative to the amount of FLS2 in WT plants.

(G) Pathogenicity assays on wild-type (WT) *Arabidopsis*, plants that overexpress ORM proteins, and RNAi lines that express low amounts of *ORM* RNA using a *Pto* DC3000 *fliC* mutant that lacks flagellin.

EV, empty vector. In **(B)** to **(F)**, Ponceau staining (PS) blots served as a loading control. The experiments were repeated three times with similar results.

FLS2-GFP and free GFP compared with control plants expressing only FLS2-GFP (Supplemental Figure 4A). We next tested whether FLS2 site-specific mutants defective in either kinase activity (FLS2$_{K898M}$) (Asai et al., 2002), ability to be ubiquitinated (FLS2$_{P1076A}$) (Salomon and Robatzek, 2006), or ability to be internalized (FLS2$_{T867V}$) (Robatzek et al., 2006) still showed reduced FLS2 levels when co-expressed with ORM1-HA or ORM2-HA. Notably, levels of FLS2$_{K898M}$ and FLS2$_{P1076A}$, but not FLS2$_{T867V}$, were reduced in the presence of ORM proteins (Supplemental Figure 4B), suggesting that FLS2 internalization, but not its kinase activity or its ability to be ubiquitinated, is required for the ORM-dependent reduction of FLS2 levels.

To evaluate the specificity of ORM-dependent reduction in FLS2 levels, we investigated whether ORM1/2 could promote the reduction in levels of other immunity-related proteins, including members of the FLS2 complex and other PRRs (Couto and Zipfel, 2016). We found that BAK1, BIK1, EFR, and LORE1 all accumulated normally when co-expressed with ORM1-HA or ORM2-HA in *N. benthamiana* (Supplemental Figure 5A). Additionally, two receptor kinases from the FLS2 subfamily (LRR-RK XII) possessing the highest (encoded by AT2G24130) and lowest (encoded by AT3G47090) sequence similarity with FLS2 accumulated to normal levels in the presence of ORM1-HA or ORM2-HA (Supplemental Figure 5B). These data suggest that ORM1/2 specifically promotes reduction of FLS2 levels but does not affect accumulation of functionally or phylogenetically related immune proteins.

ORM-Dependent Reduction in FLS2 Accumulation Is Not Due to Sphingolipids

Next, we sought to understand the mechanisms by which ORMs cause the reduction of FLS2 protein levels. Recently, it was reported that *orm1* T-DNA mutant and *ORM2* RNAi knockdown lines accumulated similar levels of sphingolipids compared with wild-type plants (Li et al., 2016). Consistent with this report, we found no significant quantitative differences in individual sphingolipid species between wild-type *Arabidopsis*, *ORM* overexpression, or *ORM* RNAi plants (Kimberlin et al., 2016). To look more closely at the relationship between ORMs and sphingolipids, we took a complementary approach, focusing on the *Arabidopsis* SPT enzyme, which catalyzes the first and rate-limiting enzymatic reaction in the sphingolipid biosynthesis pathway and is inhibited by ORMs (Kimberlin et al., 2016). We reasoned that if differences in sphingolipids caused the ORM-dependent reduction of FLS2 levels, then inactivation of SPT may also promote the reduction of FLS2 protein levels. Therefore, we inhibited SPT through use of its inhibitor, myriocin (Spassieva et al., 2002; Saucedo-Garcia et al., 2011), or through

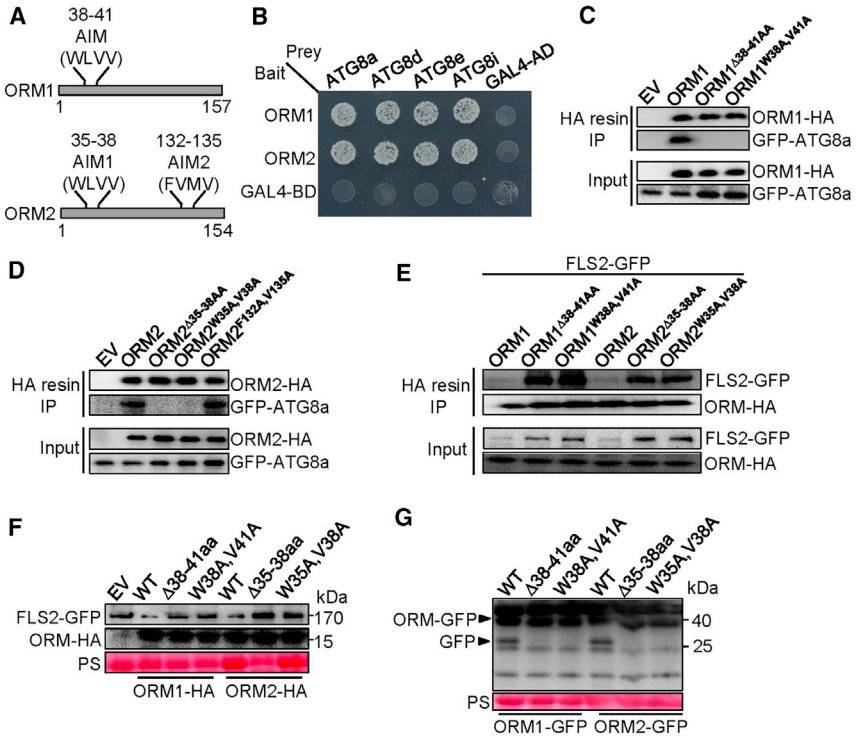

Figure 3. ORMs Interact with ATG8 and FLS2.

(A) Schematic representation of ORM1 and ORM2 containing putative ATG8 interacting motifs (AIMs). The amino acid residues corresponding to each AIM and the length of each ORM protein are indicated above and below, respectively, each protein representation.

(B) The interaction between ORM1/2 and ATG8 proteins in yeast two-hybrid assays.

(C) The putative AIM of ORM1 is required for *in vivo* interaction of ORM1 and ATG8a. Co-immunoprecipitation (IP) experiments were done using recombinant GFP-ATG8a and HA fusions of ORM1 or ORM1 AIM mutant derivatives ($ORM1_{\Delta 38\text{-}41}$ and $ORM1_{W38A,V41A}$).

(D) The N-terminal AIM, but not the C-terminal AIM, is required for ORM2's *in vivo* interaction with ATG8a. Co-immunoprecipitation experiments were performed using recombinant GFP-ATG8a and HA fusions of ORM2 or ORM2 AIM1 derivatives ($ORM2_{\Delta 35\text{-}38}$ and $ORM2_{W35A,V38A}$) or an ORM2 AIM2 mutant derivative ($ORM2_{F132A,V135A}$).

(E) Co-immunoprecipitation experiments reveal protein interaction between FLS2 and ORM AIM mutants *in vivo*. WT ORM-HA or ORM-HA AIM mutants were transiently co-expressed in *N. benthamiana* with FLS2-GFP, and co-immunoprecipitation experiments were done 3 days after *Agrobacterium* infiltration.

(F) Immunoblot analysis of FLS2-GFP when transiently co-expressed with either WT ORM-HA or ORM-HA AIM mutants defective in ATG8 interaction.

(G) Immunoblot analysis of WT ORM-GFP or ORM-GFP AIM mutants transiently expressed in *N. benthamiana*. In **(F)** and **(G)**, equal loading controls are represented by PS-stained blots.

EV, empty vector. Experiments were performed three times with similar results.

RNA silencing of its small subunit positive regulator ssSPTa—both of which are techniques that should mimic the functional consequences of ORM overexpression on sphingolipid biosynthesis (Kimberlin et al., 2013). We found that myriocin application did not affect FLS2 protein abundance or flg22-induced ROS production, despite the fact that it inhibited isotope-labeled sphingolipid biosynthesis in *Arabidopsis* suspension cultured cells from the same culture (Supplemental Figure 6A–6D).

FLS2 abundance was also not altered in the ssSPTa RNAi plants or ssSPTa overexpression plants compared with wild-type plants (Supplemental Figure 6E). To further test whether sphingolipid biosynthesis was responsible for the reduction of FLS2 levels by ORMs, we tested LOH2 overexpressing plants, which have been reported to accumulate increased levels of LCBs and C16 fatty acids (Luttgeharm et al., 2015). We also tested sphingoid base hydroxylase (*sbh*)*1* and *sbh2* knockout mutants, because both SBH1 and SBH2 function downstream of SPT and are known to produce increased sphingolipid levels (Chen et al., 2008). We detected comparable levels of FLS2 in LOH2 overexpressing lines, *sbh1* and *sbh2* mutants, and wild-type plants (Supplemental Figure 6E). Finally, we further evaluated ssSPTa RNAi and ssSPTa overexpression plants by determining the extent to which they were susceptible to *Pto* DC3000. We found these plants to be similar to wild-type *Arabidopsis* in susceptibility to *Pto* DC3000 (Supplemental Figure 6F). Taking these results together, we found no evidence that the FLS2-related phenotypes we observed for *ORM* overexpression lines, *ORM* RNAi plants, and CRISPR *orm* mutants were due to changes in sphingolipid homeostasis.

ORMs Interact with ATG8 and FLS2

In searching for a molecular mechanism that could explain the ORM-dependent reduction in FLS2 levels, we considered selective autophagy, a major cellular degradation system that sequesters and transports specific substrates into vacuoles for degradation (Farre and Subramani, 2016; Marshall and Vierstra, 2018). Recent studies found that GFP-tagged cargoes of plant selective autophagy are cleaved in the vacuole, releasing stable free GFP moieties (Li et al., 2014; Marshall et al., 2015), reminiscent of our observation for FLS2-GFP (Figure 2B and Supplemental Figure 4A). The specificity of substrates of selective autophagy is determined by selective autophagy receptors, which recruit cargoes into autophagosomes through their ability to interact with ATG8 proteins (Stolz et al., 2014). We found that ORM1 and ORM2 contain putative AIMs and therefore may be selective autophagy receptors (Figure 3A). ORM1 has a putative AIM with the consensus sequence WXXV at its N terminus, while ORM2 contains an N-terminal AIM (WXXV) and a C-terminal AIM (FXXV).

The nine *ATG8* genes in *Arabidopsis* are divided into four groups based on phylogenetic relationships (Marshall et al., 2015). In yeast two-hybrid assays using one member from each ATG8 group, ORM1 and ORM2 interacted with all ATG8s tested (ATG8a, ATG8d, ATG8e, and ATG8i) (Figure 3B). Furthermore, we found that GFP-tagged ATG8a, ATG8d, ATG8e, and ATG8i

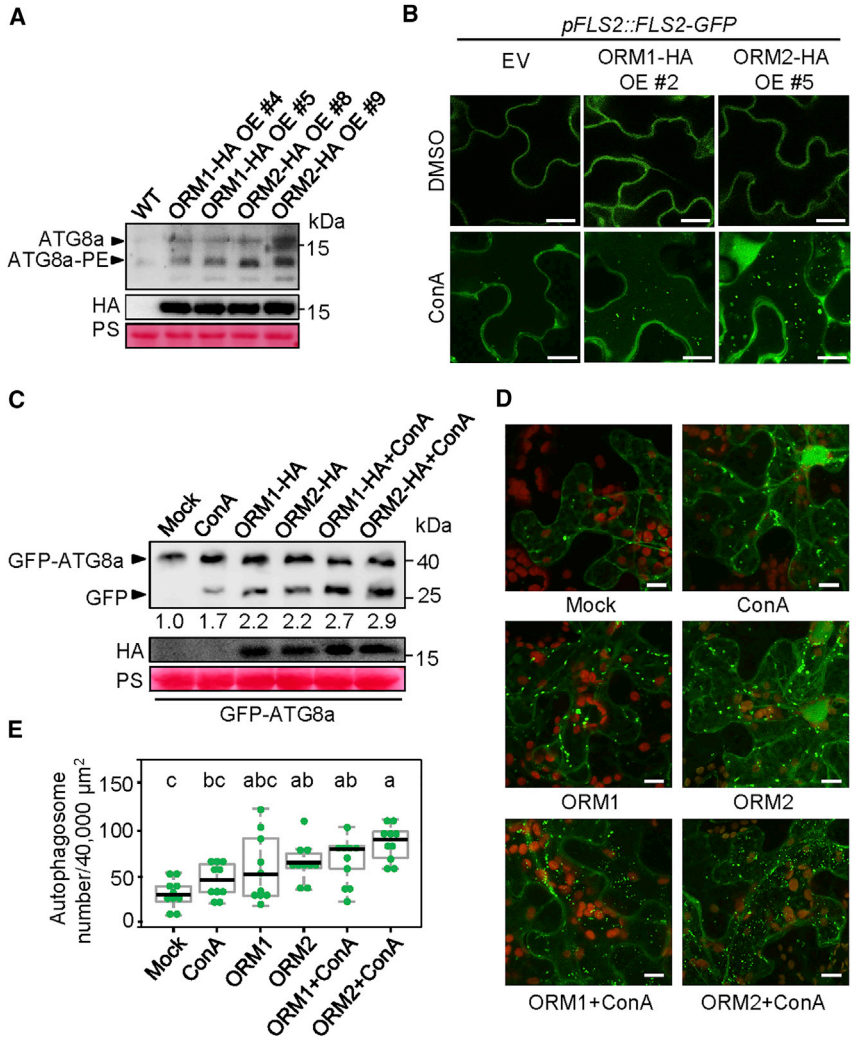

Figure 4. Overexpression of *ORMs* Induces Autophagy and Autophagosome Formation.

(A) Immunoblot analysis of ATG8a accumulation and PE modification in wild-type *Arabidopsis* (WT) and plant lines overexpressing ORM1-HA or ORM2-HA.

(B) Confocal microscopy of *Arabidopsis* FLS2-GFP plants expressing ORM1/2-HA treated with the autophagy inhibitor concanamycin A (ConA) for 18 h prior to imaging. EV, empty vector. Scale bars, 10 μm.

(C) Immunoblot analysis of GFP-ATG8a when co-expressed with ORM-HA in *N. benthamiana* in the presence or absence of ConA.

(D and E) Confocal imaging **(D)** and quantification **(E)** of GFP-ATG8a-labeled autophagosomes upon ORM overexpression in the presence or absence of ConA in *N. benthamiana*. Different letters in the graph indicate statistical significance between treatments (Tukey's HSD test; $P < 0.05$). $n = 10$ technical replicates. Scale bars, 10 μm.

Experiments were repeated three times with similar results.

immunoprecipitated with ORM1-HA or ORM2-HA when transiently co-expressed in *N. benthamiana* (Supplemental Figure 7A and 7B). To determine whether AIMs were required for ORM1 and ORM2 to interact with ATG8, we constructed two ORM1 AIM mutants: $ORM1_{\Delta 38\text{-}41}$ lacks the entire AIM, and $ORM1_{W38A,V41A}$ contains alanine substitutions of two key AIM amino acid residues. We also constructed three ORM2 AIM mutants: $ORM2_{\Delta 35\text{-}38}$ and $ORM2_{W35A,V38A}$, both containing mutations in the N-terminal AIM; and $ORM2_{F132A,V135A}$, a mutant containing site-directed mutations in the C-terminal AIM. Both ORM1 AIM mutants ($ORM1_{\Delta 38\text{-}41}$ and $ORM1_{W38A,V41A}$) lost their ability to associate with ATG8a, as did $ORM2_{\Delta 35\text{-}38}$ and $ORM2_{W35A,V38A}$; $ORM2_{F132A,V135A}$ was the only mutant able to interact with ATG8a (Figure 3C and 3D). We confirmed via bimolecular fluorescence complementation (Supplemental Figure 7C) experiments that ORM1's AIM and ORM2's N-terminal AIM were required for each ORM-ATG8 interaction. Collectively, these data suggest that both ORM1 and ORM2 can interact with ATG8 and that their respective N-terminal AIMs are required for binding ATG8.

Next, we tested whether ORM1 and ORM2 interact with FLS2. We found that ORM AIM mutants were able to immunoprecipitate FLS2-GFP when they were co-expressed in *N. benthamiana* leaves (Figure 3E). These were important findings, as hitherto we were unable to demonstrate an interaction between ORM1/2 and FLS2 because when wild-type ORM1/2 is overexpressed, FLS2 levels are diminished. Furthermore, FLS2-GFP levels were not reduced in plants expressing ORM AIM mutants that were unable to bind ATG8, suggesting that an interaction between the ORM proteins and ATG8 is required for reduction of FLS2 protein levels (Figure 3F).

Some studies reported that degradation of selective autophagy receptors could be detected with immunoblots (Svenning et al., 2011). Nevertheless, there are also the cases that degradation of autophagy receptors can not be detected by immunoblots (Lu et al., 2014). However, if the receptor was fused to GFP, an increase of the GFP moiety may be detected, suggesting that the receptor was degraded via autophagy (Marshall et al., 2015; Mochida et al., 2015). We did not observe changes in HA-tagged ORM protein abundance when ORM1 or ORM2 were transgenically or transiently expressed *in planta* (e.g., Figure 2B and 2C). However, when we performed similar experiments with GFP-ORMs in *N. benthamiana* leaves, we found that free GFP was released from full-length ORM-GFP (Figure 3G). GFP release from ORM-GFP was not observed when ORM1/2 AIM mutants were used. Thus, these results suggest that ORM proteins are degraded along with FLS2 via autophagy.

ORMs Induce ATG8 Conjugation and Autophagosome Formation

To further characterize the possible role of ORMs in selective autophagy, we tested whether ORM1 or ORM2 increases the conjugation of ATG8 to phosphatidylethanolamine (PE), which occurs during autophagosome formation (Ichimura et al., 2000). Higher levels of ATG8a and ATG8a-PE were detected in *Arabidopsis* plants overexpressing ORM1-HA or ORM2-HA than were detected in wild-type plants (Figure 4A). Moreover,

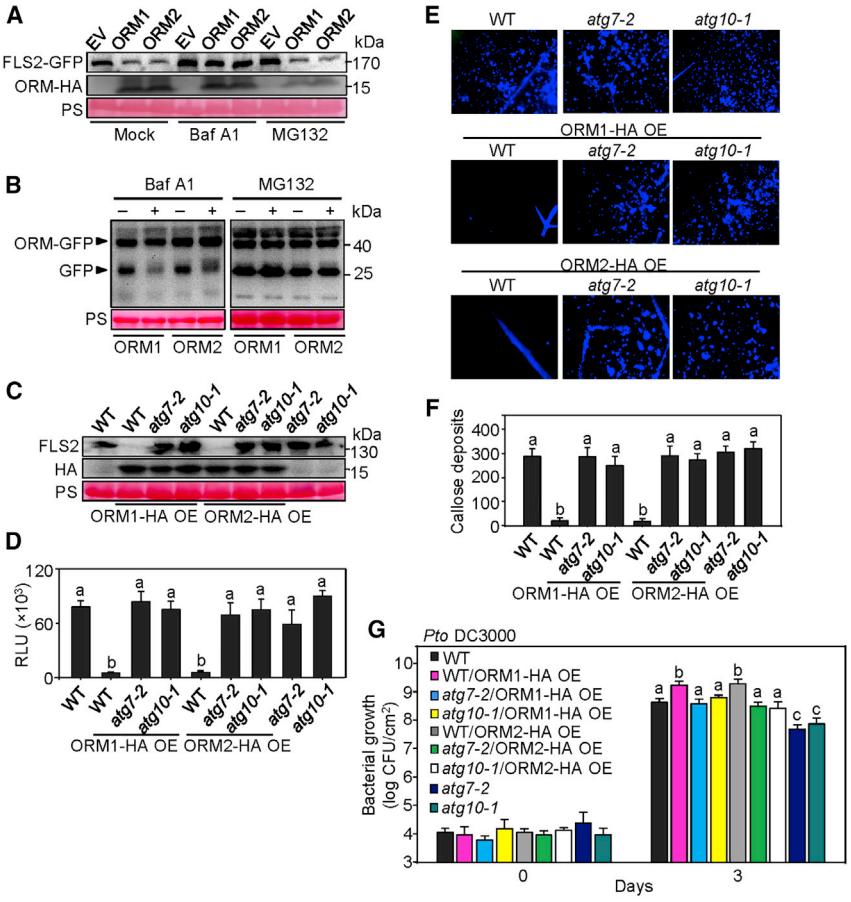

Figure 5. ORM Proteins Promote Autophagic Degradation of FLS2.

(A) Autophagy inhibitor Baf A1, but not proteasome inhibitor MG132, blocks FLS2-GFP degradation when co-expressed with ORM-HA in *N. benthamiana*.

(B) Immunoblot analysis of ORM-GFP when transiently expressed in the presence of Baf A1 and MG132.

(C) Immunoblot analysis of endogenous FLS2 in Col-0, *atg7*, *atg10*, and stable *atg7* and *atg10* transgenic lines overexpressing *ORM1-HA* or *ORM2-HA*. In **(A)** to **(C)**, PS-stained blots show equal loading.

(D) ROS production in *Arabidopsis* plants indicated in **(C)** after 1 μM flg22 treatment. Relative luminescence units (RLU) show cumulative ROS production during 30 min of treatment ($n = 12$). Different letters in the graph indicate statistical significance between treatments (one-way ANOVA with Tukey's test; $P < 0.01$).

(E and F) Visualization **(E)** and quantification **(F)** of callose deposition in response to infiltration with 1 μM flg22 in the *Arabidopsis* plants indicated in **(C)**. Values are mean ± SE, $n = 18$. Different letters in the graph indicate statistical significance between treatments (one-way ANOVA with Tukey's test; $P < 0.01$).

(G) Pathogenicity assay of plant lines in **(C)** after 3 days of *Pto* DC3000 infection. Values of bacterial growth are presented as mean ± SE. Different letters in the graph indicate statistical significance between treatments (one-way ANOVA with Tukey's test; $P < 0.01$).

EV, Empty vector; WT, wild-type. The experiments were repeated three times with similar results.

transient expression of ORM1-HA or ORM2-HA in *N. benthamiana* stimulated endogenous ATG8a and ATG8a-PE accumulation (Supplemental Figure 8).

To determine whether FLS2-GFP could be detected inside the plant vacuole during ORM-mediated FLS2 degradation, we treated FLS2-GFP ORM1/2-HA plants with concanamycin A (ConA), an autophagy inhibitor that alters the vacuolar pH and causes accumulation of autophagy cargo proteins (Marshall et al., 2015; Nolan et al., 2017). Treatment of FLS2-GFP plants overexpressing ORM1/2 with ConA resulted in dramatic accumulation of FLS2-GFP-labeled punctate foci within the vacuole, whereas control plants exhibited a low number of GFP punctate foci (Figure 4B), suggesting that FLS2-GFP is located inside the vacuole when ORM1 or ORM2 is overexpressed in plants.

Next, we tested the effects of ORMs on autophagic flux. We transiently expressed GFP-ATG8a with ORM1-HA or ORM2-HA in *N. benthamiana* in the presence of the autophagy inhibitor ConA. ConA treatment resulted in greater amounts of free GFP released from GFP-ATG8a when compared with the mock control, suggesting steady-state levels of autophagy activity (Figure 4C). Transient expression of ORM1-HA or ORM2-HA with GFP-ATG8a increased the cleavage of GFP-ATG8a. Furthermore, we observed that transiently expressing ORM1-HA or ORM2-HA enhanced the number of GFP-ATG8a-labeled punctate foci in *N. benthamiana* leaves (Figure 4D and 4E). Treatment of leaves with ConA led to an increase in the number of GFP punctate foci inside vacuoles. Collectively, these data suggest that ORMs stimulate autophagy and autophagosome formation *in planta*.

To directly determine whether reduction in FLS2 levels was due to selective autophagic degradation, we transiently expressed FLS2-GFP with ORM1-HA or ORM2-HA in *N. benthamiana* in the presence of bafilomycin A1 (Baf-A1) or MG132. Baf-A1 inhibited FLS2-GFP degradation, but levels of FLS2-GFP in the presence of MG132 were similar to those in untreated plants, suggesting that FLS2 is degraded via selective autophagy, not by the 26S proteasome (Figure 5A). We also found that Baf-A1, but not MG132, prevented autophagic degradation of ORM1/2-GFP (Figure 5B). To directly test the extent that autophagy components are necessary for ORM-mediated FLS2 degradation, we constructed *Arabidopsis* autophagy mutant plants *atg7-2* and *atg10-1* that overexpress ORM1-HA or ORM2-HA. The *atg7-2* and *atg10-1* mutants were reported to compromise the ATG8-PE conjugation process, which plays an important role in autophagosome formation (Marshall et al., 2015). Strikingly, we found that FLS2 accumulated normally in *atg7-2* and *atg10-1* mutants overexpressing ORM1/2-HA (Figure 5C), and the levels of flg22-induced ROS burst and callose deposition in these plants were also similar to those in wild-type *Arabidopsis* (Figure 5D–5F). If autophagy is the cause of the enhanced susceptibility observed in *Arabidopsis* plants overexpressing either ORM1 or ORM2, the wild-type phenotype should be restored in the *atg7-2* and *atg10* background. Indeed, enhanced susceptibility to *P. syringae* was not observed in *Arabidopsis atg7-2* and *atg10-2* mutant plants

overexpressing either ORM protein (Figure 5G). Taken together, these data suggest that ORM proteins act as selective autophagy receptors for FLS2 cargo, leading to autophagic degradation of FLS2.

DISCUSSION

Here we have presented multiple lines of evidence indicating that ORM1 and ORM2 can act as autophagy receptors for FLS2. These results were surprising, because we expected that the phenotypes associated with ORM overexpression, underexpression, or null expression were due to changes in sphingolipid homeostasis. In this study, we showed that these phenotypes were due to the absence of FLS2 in the ORM1/2 overexpression plants and elevated FLS2 levels in plants that expressed low levels of ORM1 or ORM2 (Figure 2B, 2C, 2E, and 2F). These results were confirmed by pathogenicity assays with a *P. syringae* mutant lacking flagellin, which can no longer activate FLS2. This *P. syringae* mutant also no longer exhibited enhanced growth on *Arabidopsis* plants overexpressing ORM1 or ORM2, nor did it exhibit reduced growth on *ORM1/2* RNAi plants, indicating that the *P. syringae* growth phenotypes were dependent on FLS2 activation (Figure 2G).

We proposed a model explaining the involvement of ORMs in plant immunity as follows: ORMs function as selective autophagy receptors for non-activated FLS2, inducing the degradation of small amounts of total FLS2 via selective autophagy, and thereby functioning in the maintenance of FLS2. Autophagy is activated in plants that overexpress ORM1/2, and FLS2 levels are enhanced in *Arabidopsis orm1* and *orm2* mutants. Recycling non-activated FLS2 would ensure that sufficient functional FLS2 is present to maintain FLS2 signaling. Alternatively, ORMs may regulate *de novo* FLS2 production in the ER via selective autophagy, which would be consistent with the finding that autophagosomes can mature from the ER (Zhuang et al., 2017).

It is possible that ORM proteins also function in immunity through negative regulation of sphingolipid biosynthesis as earlier proposed (Li et al., 2016). However, the mechanism of negative regulation of sphingolipid biosynthesis by ORMs is not well understood, and it is possible that ORMs exert their function on sphingolipid biosynthesis via selective autophagy. As Li et al. (2016) reported, *Arabidopsis orm1* ORM2 RNAi plants are more resistant to *P. syringae* and oxidative stress. Thus, they observed increased resistance to *P. syringae* similar to what we report here for the *ORM* RNAi plants. They concluded that the resistance to biotic and abiotic stresses was due to ER stress. However, we found that the increased resistance to *P. syringae* was dependent on FLS2 activation. One observation that might explain this discrepancy is that we were unable to isolate a viable *orm1orm2* double mutant plant, suggesting that complete functional loss of both ORMs results in lethality. The experimental plants used in Li et al. (2016) may have accumulated lower amounts of ORM proteins than the plants used in our experiments, and, because ORMs seem to be required for *Arabidopsis* viability, the plants used by Li et al. may have been generally stressed. This would require further comparative studies. Nevertheless, we show here that all the phenotypes we observed in ORM plants were specifically linked to FLS2 signaling.

In this study we have presented compelling evidence suggesting that ORM1/2 are selective autophagy receptors and that FLS2 is degraded via autophagy. Firstly, we showed that ORM1/2 interacted with ATG8 in an AIM-dependent manner. ORM1/2 site-directed mutants, in which conserved amino acids within the AIMs were substituted with alanine, no longer interacted with ATG8, , whereas they interacted with the FLS2 cargo. This ORM-FLS2 interaction is difficult to be detected in plants expressing wild-type ORM1/2, likely because FLS2 levels are greatly diminished. Second, we demonstrated that autophagy inhibitors and *Arabidopsis* mutants defective in autophagy stabilize FLS2 protein levels in plants that overexpress ORMs. We also showed that FLS2-GFP is observed inside plant vacuoles as GFP-labeled foci resembling autophagosomes in plants treated with ConA. Finally, we found that *P. syringae* growth levels are restored to wild-type levels in *Arabidopsis atg* mutants that overexpress ORMs. If ORMs act as selective autophagy receptors, then these proteins are either multifunctional or are negatively regulating sphingolipid biosynthesis through selective autophagy. Interestingly, putative AIMs are also present in human and mouse ORMs but not in yeast ORMs (Supplemental Figure 9), raising the possibility that ORMs generally act as selective autophagy receptors in other eukaryotes.

Activated FLS2 is degraded via the 26*S* proteasome (Lu et al., 2011), but this event is distinct from the FLS2 autophagic degradation we observed. However, it is important to note that we did not test how activated FLS2 behaves in plants over- or underexpressing ORM proteins. Plant immunity has been linked previously to autophagy, mostly through association with the hypersensitive response, a programmed cell death linked to immunity (Liu et al., 2005; Patel and Dinesh-Kumar, 2008; Hofius et al., 2009). Our results as well as a previous report (Lenz et al., 2011) revealed that *Arabidopsis atg* mutants are more resistant to *P. syringae* infection, but flg22-triggered ROS production and callose deposition are unaffected (Figure 5D–5G). Moreover, FLS2 accumulation in *atg* mutants was not significantly different from that in wild-type plants (Figure 5C). These results clearly show that ORM-dependent FLS2 degradation and the enhanced bacterial resistance of *atg* mutant plants are both impaired when ORMs are overexpressed, suggesting an important role for ORMs in autophagy-dependent plant immunity.

Recently, selective autophagy has been shown to be either proviral or antiviral, depending on the virus (Hafren et al., 2017; Haxim et al., 2017), and to be involved in *P. syringae* pathogenesis (Ustun et al., 2018). Interestingly, a virulence effector from the plant pathogen *Phytophthora* has been shown to compete with a host-selective autophagy receptor to the benefit of the pathogen (Dagdas et al., 2016). The cargo for this autophagy receptor is not currently known. Indeed, in *Arabidopsis* many autophagy receptors have been identified, but for most of them the corresponding cargo has remained unidentified (Marshall and Vierstra, 2018). Our results suggest that selective autophagy plays a maintenance role in plant immunity and opens up the possibility that other immune receptors may act as cargo for ORM proteins or other selective autophagy receptors. Moreover, our results suggest a broader role for ORM proteins beyond regulation of sphingolipid biosynthesis.

METHODS

Plant Materials and Growth Condition

The *A. thaliana* Col-0 *ORM1* RNAi, ORM1 overexpression, *ORM2* RNAi, and ORM2 overexpression lines we used were previously reported (Kimberlin et al., 2016). We generated transgenic plants overexpressing ORM1/2 in these other plant backgrounds: wild-type *A. thaliana* Col-0, Col-0 (*FLS2p*::*FLS2-3*×*myc-GFP*) (Robatzek et al., 2006); Col-0 *atg7-2* (CS369834) (Marshall et al., 2015); and *atg10-1* (Salk_084434) (Marshall et al., 2015). The pBinGlyRed-35S-derived binary constructs pLN6222 and pLN6223 containing *ORM1-HA* and *ORM2-HA*, respectively, were transformed into *Agrobacterium tumefaciens* C58C1 by electroporation. In addition, we made transgenic wild-type *A. thaliana* Col-0 plants expressing either ORM1-HA or ORM2-HA under the control of an estradiol-inducible promoter using the binary vector pER8 (Zuo et al., 2000). All transgenic plants were generated by the floral dipping method (Clough and Bent, 1998). For pBinGlyRed-35S-derived plants, transformed seeds were identified using a green LED light with a Red 2 camera filter to detect fluorescence of DsRed-marked proteins. Basta was used to screen for pER8-transformed seeds as described by Zuo et al. (2000). We made ten independent transgenic lines for each construct. The *A. thaliana ssSPTa* RNAi and ssSPTa overexpression lines and *sbh1* and *sbh2* T-DNA mutants were previously reported (Chen et al., 2008; Kimberlin et al., 2013). All *Arabidopsis* plants were grown at 25°C with a 12:12-h photoperiod in growth chambers. *N. benthamiana* plants were grown at room temperature in standard greenhouses.

Agrobacterium-Mediated Transient Gene Expression in *N. benthamiana*

Agrobacterium transient gene expression assays were carried out as described by Guo et al. (2016). For co-expression, pairs of *Agrobacterium* strains, each containing a binary construct, at an OD_{600} of 0.5, were mixed in a 1:1 ratio and infiltrated into 5-week-old *N. benthamiana* leaves.

Chemical Treatments

N. benthamiana leaves co-expressing FLS2-GFP and ORM1/2-HA were infiltrated with 2 μM autophagy inhibitor Baf-A1 (Sigma) (Lu et al., 2014) or 10 μM proteasome inhibitor MG132 (Sigma) (Lu et al., 2011); DMSO was infiltrated as a control. FLS2-GFP abundance was determined by immunoblotting 48 h after the Baf A1 or MG132 treatments. To determine whether the GFP-ATG8a-labeled punctate structure is an autophagosome, we infiltrated 1 μM concanamycin A (ConA) (Sigma) into *N. benthamiana* leaves co-expressing GFP-ATG8. Imaging with standard confocal microscopy was done 16 h after the ConA treatment. To determine the effects of SPT on immune defenses, we infiltrated *Arabidopsis* Col-0 leaves using a needleless syringe with 5 μM SPT inhibitor myrocin or DMSO as a control as previously reported (Spassieva et al., 2002). Leaves were harvested 18 h post chemical infiltration for the ROS assay.

Co-immunoprecipitation and Immunoblotting

After *Agrobacterium* infiltration, transgenic *Arabidopsis* or *N. benthamiana* leaves were ground with one volume of extraction buffer as described by Lu et al. (2011) (10 mM HEPES [pH 7.5], 100 mM NaCl, 1 mM EDTA, 10% glycerol, 0.5% Triton X-100, and protease inhibitor cocktail from Roche). Samples were vortexed and centrifuged at 15 000 rpm for 10 min at 4°C. Supernatants were taken for protein quantification using the Bradford assay. For the co-immunoprecipitation assay, the same volume of supernatant with the same amount of protein was incubated with anti-HA affinity matrix resin (Roche) for 4 h at 4°C with gentle rotation. Equal amounts of protein from each sample were subjected to standard SDS–PAGE and immunoblotting analysis. For ATG8a analysis, equal amounts of proteins were subjected to SDS–PAGE with 6 M urea (Hofius et al., 2009). The polyclonal antibody against FLS2 (ag1857) was purchased from Agrisera. Polyclonal antibodies against GFP (ab6556), ATG8a (ab77003), and ubiquitin (ab7254) were purchased from Abcam. The monoclonal antibody against HA (11867423001) was purchased from Sigma.

Pathogenicity Assay in *Arabidopsis*

Bacterial growth *in planta* was measured as described by Guo et al. (2016). Four-week-old *Arabidopsis* plants were blunt-syringe infiltrated with 1×10^5 cells ml^{-1} of wild-type *Pto* DC3000 or *Pto* DC3000 Δ*hrcC* suspended in $MgCl_2$. The inoculated plants were incubated in a growth chamber with a 12-h light cycle at 25°C with humidity. Bacterial populations were assessed at the indicated times. Four 0.3-cm^2 leaf disks from infiltrated leaves were harvested with a cork borer and ground in dH_2O. Serial dilutions were spotted on King's B medium agar plates containing the appropriate antibiotics. Plates were incubated at 25°C for 2 days to calculate the number of cells per cm^2.

Measurement of ROS Production

The ROS assay was performed as described by Guo et al. (2016). In brief, 10 leaf disks from each *Arabidopsis* line were sampled with a cork borer and incubated into 100 μl of dH_2O in a 96-well plate. The following day, dH_2O was replaced with reaction buffer containing 1 μM flg22, 1 μM elf18, or 100 μg/ml chitin. The intensity of ROS production was measured by counting photons from L-012-mediated luminescence.

Visualization and Quantification of Callose Deposits

Four-week-old *Arabidopsis* plants were infiltrated using a needleless syringe with 1 μM flg22, 1 μM elf18, or 100 μg/ml chitin. At 18 h post infiltration, leaves were incubated with ethanol to eliminate chlorophyll and stained with aniline blue. Callose deposits were visualized and quantified as reported previously (Guo et al., 2016).

Yeast Two-Hybrid Assay

Wild-type and AIM1 mutant *ORM2* sequences were cloned into pDEST™22 vectors carrying the GAL4 activation domain. *ATG8a*, *ATG8d*, *ATG8e*, and *ATG8i* genes were amplified and introduced into pDEST™32 vectors containing the GAL4 binding domain. The resulting plasmids were paired and co-transformed into *Saccharomyces cerevisiae* MaV203 cells; empty vectors were included as controls. Cells transformed with both plasmids were selected on synthetic complete (SC) medium (lacking leucine and tryptophan). Protein interactions were identified by growing selected yeast cells on SC medium (lacking leucine, tryptophan, and histidine) containing 50 mM 3-amino-1,2,4-triazole.

Quantitative RT–PCR Analysis

Total RNA was extracted from 4-week-old *Arabidopsis* plants using the RNeasy Plant Mini Kit (Qiagen) following the manufacturer's instructions. qPCR assays of *FRK1*, *WRKY29*, and *FLS2* expression were performed using the iTaq Universal SYBR Kit (Bio-Rad) with actin expression as the internal standard.

Bimolecular Fluorescence Complementation Assay

The sequence encoding the C-terminal half of YFP was fused to the ATG8a coding sequence by PCR, and the resulting sequence, ATG8a-cYFP, was introduced into the binary vector pPZP212. The sequence encoding the N-terminal half of YFP was fused to wild-type ORM or ORM AIM mutant coding sequences by PCR, and the fused fragments were each introduced into the binary vector pPZP212. Pairs of Agrobacterium strains carrying binary vectors were mixed in a 1:1 ratio (OD_{600} = 0.5) and infiltrated into 5-week old *N. benthamiana* leaves. Confocal microscope images were taken 48 h after agroinfiltration.

Visualization and Quantification of ATG8-Labeled Autophagosomes

Autophagosome assays were performed as previously described (Dagdas et al., 2016), with minor modifications. Half of the *N. benthamiana* leaves were agroinfiltrated with constructs for transient expression of either GFP-ATG8a alone or GFP-ATG8a plus HA-ORM. Following incubation for

48 h, leaves expressing GFP-ATG8a/HA-ORM were infiltrated with the autophagy inhibitor ConA or an equivalent volume of DMSO as a control. Leaves expressing GFP-ATG8a alone were infiltrated with the same volume of DMSO. Confocal microscope images were taken 5–10 h after chemical application. Each sample consisted of five independent biological replicates. Each replicate was scanned twice by a Nikon A1 confocal system to generate z sections with 60 images each. To quantify autophagosome formation, we opened individual images from each z section with Fuji ImageJ. The GFP-ATG8a-labeled punctate structures were counted using the menu Plugins/Analyze/Cell counter.

Generation of *orm1* and *orm2* Mutants Using CRISPR/Cas9

Target sites of ORM1 and target sites of ORM2 fused with a single guide RNA (sgRNA) were introduced into the CRISPR/Cas9 binary vector pHEE2E to generate pHEE2E-ORM1 and pHEE2E-ORM2, respectively, following a previously reported method (Wang et al., 2015). We electroporated the pHEE2E-ORM vectors into *Agrobacterium* strain GV3101 and transformed *Arabidopsis* Col-0 wild-type plants via the floral dip method. The collected seeds were screened for hygromycin resistance on Murashige and Skoog plates. We amplified fragments surrounding the target regions of ORM1 and ORM2 from the genomic DNA of transgenic plants and performed a restriction enzyme digestion assay. The Cas9-induced site-specific indels were identified by DNA sequencing.

Measurement of the Effects of Myriocin on Sphingolipid Synthesis

A. thaliana Col-0 suspension cultured T87 cells were grown in NT-1 medium containing stable isotope nitrogen 15 (ammonium nitrate $NH_4{}^{15}NO_3$, potassium nitrate $K^{15}NO_3$), and the incorporation of ^{15}N into sphingolipids was tracked. The cells were treated with 1 or 5 μM myriocin or DMSO as a mock control. The cells were maintained under continuous illumination (100 μmol m^{-2} s^{-1}) at 22°C with shaking at 120 rpm. The cells were sampled 0 h and 18 h after chemical treatments. A small portion of cells from each treatment were used for immunoblotting. Sphingolipids were extracted from the remainder of cells and analyzed as described by Markham and Jaworski (2007). The mass changes of ^{15}N-labeled sphingolipid species were measured by mass spectrometry.

SUPPLEMENTAL INFORMATION

Supplemental Information is available at *Molecular Plant Online*.

FUNDING

This research was supported by grant no. MCB-1158500 and grant no. MCB-1818297 from the National Science Foundation (to E.B.C.), grant no. 2014-67013-21721 from the United States Department of Agriculture National Institute of Food and Agriculture (to J.R.A.), and an internal grant from the Agricultural Research Division of the Institute of Agriculture and Natural Resources at the University of Nebraska (to J.R.A. and E.B.C.).

AUTHOR CONTRIBUTIONS

F.Y., E.B.C., and J.R.A. designed the experiments. A.N.K. generated untagged ORM1/2 overexpressing and *ORM1/2* RNAi transgenic *Arabidopsis* plants. Y.L. generated *orm* CRISPR/Cas9 mutant plants. A.G.-S. performed the myriocin sphingolipid inhibition experiment with suspension cultured cells. C.G.E. took the confocal microscopy images. F.Y. generated all other plant materials and performed all other experiments. F.Y. and J.R.A. wrote the manuscript.

ACKNOWLEDGMENTS

We thank members of the Alfano and Cahoon laboratories for fruitful discussions regarding the experiments described in this paper, and E. Banset for editing. We thank Drs. S. Robatzek and A. Heese for providing seed for *Arabidopsis* expressing FLS2-GFP. We thank R. Cahoon for profiling *Arabidopsis* sphingolipids. No conflict of interest declared.

Received: May 2, 2018
Revised: October 16, 2018
Accepted: November 22, 2018
Published: November 29, 2018

REFERENCES

Asai, T., Tena, G., Plotnikova, J., Willmann, M.R., Chiu, W.-L., Gomez-Gomez, L., Boller, T., Ausubel, F.M., and Sheen, J. (2002). MAP kinase signalling cascade in *Arabidopsis* innate immunity. Nature **415**:977–983.

Beck, M., Zhou, J., Faulkner, C., MacLean, D., and Robatzek, S. (2012). Spatio-temporal cellular dynamics of the *Arabidopsis* flagellin receptor reveal activation status-dependent endosomal sorting. Plant Cell **24**:4205–4219.

Breslow, D.K., Collins, S.R., Bodenmiller, B., Aebersold, R., Simons, K., Shevchenko, A., Ejsing, C.S., and Weissman, J.S. (2010). Orm family proteins mediate sphingolipid homeostasis. Nature **463**:1048–1053.

Chen, M., Markham, J.E., Dietrich, C.R., Jaworski, J.G., and Cahoon, E.B. (2008). Sphingolipid long-chain base hydroxylation is important for growth and regulation of sphingolipid content and composition in *Arabidopsis*. Plant Cell **20**:1862–1878.

Clough, S.J., and Bent, A.F. (1998). Floral dip: a simplified method for Agrobacterium-mediated transformation of *Arabidopsis thaliana*. Plant J. **16**:735–743.

Couto, D., and Zipfel, C. (2016). Regulation of pattern recognition receptor signalling in plants. Nat. Rev. Immunol. **16**:537–552.

Dagdas, Y.F., Belhaj, K., Maqbool, A., Chaparro-Garcia, A., Pandey, P., Petre, B., Tabassum, N., Cruz-Mireles, N., Hughes, R.K., Sklenar, J., et al. (2016). An effector of the Irish potato famine pathogen antagonizes a host autophagy cargo receptor. Elife **5**. https://doi.org/10.7554/eLife.10856.

Dang, J., Bian, X., Ma, X., Li, J., Long, F., Shan, S., Yuan, Q., Xin, Q., Li, Y., Gao, F., et al. (2017). ORMDL3 facilitates the survival of splenic B cells via an ATF6alpha-endoplasmic reticulum stress-Beclin1 autophagy regulatory pathway. J. Immunol. **199**:1647–1659.

Das, S., Miller, M., and Broide, D.H. (2017). Chromosome 17q21 genes ORMDL3 and GSDMB in asthma and immune diseases. Adv. Immunol. **135**:1–52.

Farre, J.C., and Subramani, S. (2016). Mechanistic insights into selective autophagy pathways: lessons from yeast. Nat. Rev. Mol. Cell Biol. **17**:537–552.

Guo, M., Kim, P., Li, G., Elowsky, C.G., and Alfano, J.R. (2016). A bacterial effector co-opts calmodulin to target the plant microtubule network. Cell Host Microbe **19**:67–78.

Hafren, A., Macia, J.L., Love, A.J., Milner, J.J., Drucker, M., and Hofius, D. (2017). Selective autophagy limits cauliflower mosaic virus infection by NBR1-mediated targeting of viral capsid protein and particles. Proc. Natl. Acad. Sci. U S A **114**:E2026–E2035.

Han, S., Lone, M.A., Schneiter, R., and Chang, A. (2010). Orm1 and Orm2 are conserved endoplasmic reticulum membrane proteins regulating lipid homeostasis and protein quality control. Proc. Natl. Acad. Sci. U S A **107**:5851–5856.

Haxim, Y., Ismayil, A., Jia, Q., Wang, Y., Zheng, X., Chen, T., Qian, L., Liu, N., Wang, Y., Han, S., et al. (2017). Autophagy functions as an antiviral mechanism against geminiviruses in plants. Elife **6**. https://doi.org/10.7554/eLife.23897.

Hofius, D., Schultz-Larsen, T., Joensen, J., Tsitsigiannis, D.I., Petersen, N.H., Mattsson, O., Jorgensen, L.B., Jones, J.D., Mundy, J., and Petersen, M. (2009). Autophagic components contribute to hypersensitive cell death in *Arabidopsis*. Cell **137**:773–783.

Ichimura, Y., Kirisako, T., Takao, T., Satomi, Y., Shimonishi, Y., Ishihara, N., Mizushima, N., Tanida, I., Kominami, E., Ohsumi, M., et al. (2000). A ubiquitin-like system mediates protein lipidation. Nature **408**:488–492.

Kimberlin, A.N., Han, G., Luttgeharm, K.D., Chen, M., Cahoon, R.E., Stone, J.M., Markham, J.E., Dunn, T.M., and Cahoon, E.B. (2016). ORM expression alters sphingolipid homeostasis and differentially affects ceramide synthase activity. Plant Physiol. **172**:889–900.

Kimberlin, A.N., Majumder, S., Han, G., Chen, M., Cahoon, R.E., Stone, J.M., Dunn, T.M., and Cahoon, E.B. (2013). *Arabidopsis* 56-amino acid serine palmitoyltransferase-interacting proteins stimulate sphingolipid synthesis, are essential, and affect mycotoxin sensitivity. Plant Cell **25**:4627–4639.

Koberlin, M.S., Snijder, B., Heinz, L.X., Baumann, C.L., Fauster, A., Vladimer, G.I., Gavin, A.C., and Superti-Furga, G. (2015). A conserved circular network of coregulated lipids modulates innate immune responses. Cell **162**:170–183.

Kunze, G., Zipfel, C., Robatzek, S., Niehaus, K., Boller, T., and Felix, G. (2004). The N terminus of bacterial elongation factor Tu elicits innate immunity in *Arabidopsis* plants. Plant Cell **16**:3496–3507.

Lenz, H.D., Haller, E., Melzer, E., Kober, K., Wurster, K., Stahl, M., Bassham, D.C., Vierstra, R.D., Parker, J.E., Bautor, J., et al. (2011). Autophagy differentially controls plant basal immunity to biotrophic and necrotrophic pathogens. Plant J. **66**:818–830.

Li, F., Chung, T., and Vierstra, R.D. (2014). AUTOPHAGY-RELATED11 plays a critical role in general autophagy- and senescence-induced mitophagy in *Arabidopsis*. Plant Cell **26**:788–807.

Li, J., Yin, J., Rong, C., Li, K.E., Wu, J.X., Huang, L.Q., Zeng, H.Y., Sahu, S.K., and Yao, N. (2016). Orosomucoid proteins interact with the small subunit of serine palmitoyltransferase and contribute to sphingolipid homeostasis and stress responses in *Arabidopsis*. Plant Cell **28**:3038–3051.

Liu, Y., Schiff, M., Czymmek, K., Talloczy, Z., Levine, B., and Dinesh-Kumar, S.P. (2005). Autophagy regulates programmed cell death during the plant innate immune response. Cell **121**:567–577.

Lu, D., Lin, W., Gao, X., Wu, S., Cheng, C., Avila, J., Heese, A., Devarenne, T.P., He, P., and Shan, L. (2011). Direct ubiquitination of pattern recognition receptor FLS2 attenuates plant innate immunity. Science **332**:1439–1442.

Lu, K., Psakhye, I., and Jentsch, S. (2014). Autophagic clearance of polyQ proteins mediated by ubiquitin-Atg8 adaptors of the conserved CUET protein family. Cell **158**:549–563.

Luttgeharm, K.D., Chen, M., Mehra, A., Cahoon, R.E., Markham, J.E., and Cahoon, E.B. (2015). Overexpression of *Arabidopsis* ceramide synthases differentially affects growth, sphingolipid metabolism, programmed cell death, and mycotoxin resistance. Plant Physiol. **169**:1108–1117.

Ma, X., Qiu, R., Dang, J., Li, J., Hu, Q., Shan, S., Xin, Q., Pan, W., Bian, X., Yuan, Q., et al. (2015). ORMDL3 contributes to the risk of atherosclerosis in Chinese Han population and mediates oxidized low-density lipoprotein-induced autophagy in endothelial cells. Sci. Rep. **5**:17194.

Markham, J.E., and Jaworski, J.G. (2007). Rapid measurement of sphingolipids from *Arabidopsis thaliana* by reversed-phase high-performance liquid chromatography coupled to electrospray ionization tandem mass spectrometry. Rapid Commun. Mass Spectrom. **21**:1304–1314.

Marshall, R.S., Li, F., Gemperline, D.C., Book, A.J., and Vierstra, R.D. (2015). Autophagic degradation of the 26S proteasome is mediated by the dual ATG8/ubiquitin receptor RPN10 in *Arabidopsis*. Mol. Cell **58**:1053–1066.

Marshall, R.S., and Vierstra, R.D. (2018). Autophagy: the master of bulk and selective recycling. Annu. Rev. Plant Biol. **69**:173–208.

Michaeli, S., Galili, G., Genschik, P., Fernie, A.R., and Avin-Wittenberg, T. (2016). Autophagy in plants—what's new on the menu? Trends Plant Sci. **21**:134–144.

Mochida, K., Oikawa, Y., Kimura, Y., Kirisako, H., Hirano, H., Ohsumi, Y., and Nakatogawa, H. (2015). Receptor-mediated selective autophagy degrades the endoplasmic reticulum and the nucleus. Nature **522**:359–362.

Nolan, T.M., Brennan, B., Yang, M., Chen, J., Zhang, M., Li, Z., Wang, X., Bassham, D.C., Walley, J., and Yin, Y. (2017). Selective autophagy of BES1 mediated by DSK2 balances plant growth and survival. Dev. Cell **41**:33–46.e7.

Patel, S., and Dinesh-Kumar, S.P. (2008). *Arabidopsis* ATG6 is required to limit the pathogen-associated cell death response. Autophagy **4**:20–27.

Robatzek, S., Chinchilla, D., and Boller, T. (2006). Ligand-induced endocytosis of the pattern recognition receptor FLS2 in *Arabidopsis*. Genes Dev. **20**:537–542.

Salomon, S., and Robatzek, S. (2006). Induced endocytosis of the receptor kinase FLS2. Plant Signal. Behav. **1**:293–295.

Saucedo-Garcia, M., Guevara-Garcia, A., Gonzalez-Solis, A., Cruz-Garcia, F., Vazquez-Santana, S., Markham, J.E., Lozano-Rosas, M.G., Dietrich, C.R., Ramos-Vega, M., Cahoon, E.B., et al. (2011). MPK6, sphinganine and the *LCB2a* gene from serine palmitoyltransferase are required in the signaling pathway that mediates cell death induced by long chain bases in *Arabidopsis*. New Phytol. **191**:943–957.

Spassieva, S.D., Markham, J.E., and Hille, J. (2002). The plant disease resistance gene *Asc-1* prevents disruption of sphingolipid metabolism during AAL-toxin-induced programmed cell death. Plant J. **32**:561–572.

Stolz, A., Ernst, A., and Dikic, I. (2014). Cargo recognition and trafficking in selective autophagy. Nat. Cell Biol. **16**:495–501.

Svenning, S., Lamark, T., Krause, K., and Johansen, T. (2011). Plant NBR1 is a selective autophagy substrate and a functional hybrid of the mammalian autophagic adapters NBR1 and p62/SQSTM1. Autophagy **7**:993–1010.

Ustun, S., Hafren, A., Liu, Q., Marshall, R.S., Minina, E.A., Bozhkov, P.V., Vierstra, R.D., and Hofius, D. (2018). Bacteria exploit autophagy for proteasome degradation and enhanced virulence in plants. Plant Cell **30**:668–685.

Wang, Z.P., Xing, H.L., Dong, L., Zhang, H.Y., Han, C.Y., Wang, X.C., and Chen, Q.J. (2015). Egg cell-specific promoter-controlled CRISPR/Cas9 efficiently generates homozygous mutants for multiple target genes in *Arabidopsis* in a single generation. Genome Biol. **16**:144.

Wong, Y.S., and Maclachlan, G.A. (1980). 1,3-beta-d-glucanases from *Pisum sativum* seedlings: III. Development and distribution of endogenous substrates. Plant Physiol. **65**:222–228.

Zhuang, X., Chung, K.P., Cui, Y., Lin, W., Gao, C., Kang, B.H., and Jiang, L. (2017). ATG9 regulates autophagosome progression from the endoplasmic reticulum in *Arabidopsis*. Proc. Natl. Acad. Sci. U S A **114**:E426–E435.

Zuo, J., Niu, Q., and Chua, N. (2000). An estrogen receptor-based transactivator XVE mediates highly inducible gene expression in transgenic plants. Plant J. **24**:265–273.